

The Role of Bio-Extracted Reduced Graphene Oxide in the Crystallization Kinetics of Chitosan Bio-Polymer

Solomon L Joseph¹, Agumba O John^{2*} and Fanuel M Keheze³

¹Department of Metrology, Kenya Bureau of Standards, P. O. Box 54974-00200, Nairobi, Kenya

²Department of Physical Sciences, Jaramogi Oginga Odinga University of Science and Technology (JOUST), P.O. Box 210-40601, Bondo, Kenya

³Department of Physics, Pwani University, P. O. Box 195-80108, Kilifi, Kenya

ABSTRACT

Carbon nanomaterials have recently attracted wide scientific applications due to their tunable properties. These novel materials act as best fillers that can provide substantial benefits due to their high strength, thermal conductivity, and electrical conductivities. With their huge applications as bulk materials, when implemented in polymer matrix as fillers, they give rise to new promising materials with which their properties can be tuned to suit a particular application. Besides the development of these new nanocomposite materials, there exist some challenges which must be fully surpassed to explore the potentiality of application of carbon-based nanocomposites. Reduced graphene oxide is one of the carbon derivatives which has attracted the current advancement in technology, and recently, it found its new applications in super capacitors used in electronic industries. The limiting factor for its exploration is the affordability. New and affordable sources of these graphene-based nanomaterial have to be devised, for fully realization of their potential applications. In this study, reduced graphene oxide and the bio-polymer chitosan were extracted from the locally available bio waste materials. Nanocomposites were prepared at 50% rGO: chitosan ratio. The films were then prepared by spin coating method. Prepared films were subjected to morphological analysis. From the results, it was observed that rGO induced chitosan crystallization, which led to formation of dendritic structures. Cellulose nanocrystals have thus displayed temperature dependent positive uniaxial birefringence.

*Corresponding author

Agumba O John, Department of Physical Sciences, Jaramogi Oginga Odinga University of Science and Technology (JOUST), P.O. Box 210-40601, Bondo, Kenya; E-mail: agumba.john@gmail.com

Received: January 12, 2021; **Accepted:** January 21, 2021; **Published:** January 29, 2021

Keywords: Chitin, Reduced Graphene Oxide Chitosan, Crystallization, Birefringence, Polymerization, Polytetrafluoroethylene

Introduction

The application of polymers in optical industry has not been optimally achieved due to presence of crystal imperfections and disorders which are brought about during the polymerization process [1-3]. The optical properties of polymers are directly dependent on the morphological order and assembly of the polymer chains [4]. Molecular ordering of the polymer chains via crystallization is one great way of improving the applications of polymers in optical industries. Crystallization of polymers has been one of the most important aspects of polymer science [5]. It is clear that the physical and optical properties of polymers are directly related to chain conformation and crystallinity order. Ancient studies of polymer crystallization mainly focused on the resulting crystalline structure and the morphology of crystals composed of low molecular weight polymers [6]. Theories on polymer crystallization were initially brought about by adapting theories that were already developed, which were used to describe crystallization of polymers with smaller molecular number. However, the main differences between those materials and long-chain polymers often led to unsatisfactory results in terms of the

shape, size and stability of the resulting polymer crystals [7].

In polymers, one can grow crystals from undercooled melts or solutions [8]. Not only simple polymers containing linear polymer structures like polyethylene (PE) and polystyrene (PS) can crystallize, but also complex ones containing complex polymeric structures which crystallizes after induced nucleation. Usually, it is not possible to obtain a 100% crystalline polymer via crystallization process. The crystallinity index of crystalline polymers ranges from about 10% to almost 80%, implying that a crystalline polymer still contains a certain amount of amorphous structures [9]. The characteristics of a crystalline polymer are related not only to the crystallinity, but also to the preferential orientation of the crystals. Since the physical properties of polymers are directly related to chain conformation and crystalline order, then crystallization of polymers changes all physical characteristics like mechanical properties. Chitosan (a partially N-deacetylated derivative of Chitin) is a polysaccharide consisting of D-glucosamine and N-acetyl-glucosamine units, connected via β -(1 \rightarrow 4) glycosidic linkages, derived from Chitin via deacetylation process [10]. Deacetylation of chitin can be approached by several methods, such as alkaline deacetylation [11], enzymatic deacetylation [10], intermittent water washing, flash solvent and organic solvents deacetylation methods [11].

Among all the above mentioned ways, alkaline deacetylation is the most commonly used [12]. The deacetylation process does away with the acetyl groups ($-\text{COCH}_3$) in N-acetyl-D-glucosamine units in Chitin and converts it to D-glucosamine units with no amine groups ($-\text{NH}_2$) to form Chitosan products that are highly soluble in selective weak organic acids due to its relatively high reactivity as compared to the chitin [13]. Chitosan chains are highly entangled, thus, a strong nucleation agent is required to induce its crystallization.

Carbon nanomaterials provides a wide range of applications in a variety of roles, including reinforcing materials, thermal and electrical conductors, and in optical absorbers. Earlier research revealed that carbon-based materials are able to induce polymer crystallization when blended with polymers. Among all the carbon materials, graphene sheets have the strongest interaction with most Polyethylene matrix. These material acts as a nucleation agents, which is the initial stage of crystallization process [14]. The interest in graphene based materials in blending and doping of polymers is also supported by its remarkable electronic properties, which makes it a potential in electrical applications. Graphene has high crystal quality, ballistic transport of electrons on a submicron scale (even under ambient conditions) and its charge carriers accurately mimic massless Dirac fermions [15]. Their applications in polymer crystallization is limited due to its high production cost. New and affordable means of obtaining rGO from locally available biomass wastes have to be developed, and its potential applications in polymer crystallization be investigated. This research was aimed at realization of the potential application rGO extracted locally from coconut husk, which may act as a cheap and alternative source of this material.

Equipment, Materials and Methods

In this study, the materials used were extracted from the locally available biomass wastes. rGO was obtained via thermal pyrolysis of coconut husks, while chitosan was extracted from squid gladii via chemical synthesis. The micrographs were taken using the Zeiss Axio 100 microscope fitted with LCD camera purchased from the Carl Zeiss AG group (Germany).

Reduced Graphene Oxide Synthesis

rGO was obtained via thermal decomposition of coconut husks biomass waste in limited air supply. The husks were cleaned using running water, to remove external dirt and dust. This was followed by sun drying for four days. The dried husks were further dried in a hot air oven at about 60°C for 6 hours. The dry husks were grounded into fine powder (1.5 mm). 15 g of the powder was put in a crucible, covered with crucible lid and then wrapped in three layers of aluminum foil to prevent oxidation during the carbonation process. The wrapped samples were put in a hot furnace at about 100°C for 5 hours [16]. A black powder, graphite, was obtained. The graphite powder was oxidized thermally in a 500°C hot furnace for 5 hours to obtain brownish powder, reduced graphite oxide. 0.1 g of the powder was mixed with 10 ml distilled water in a glass vial. The mixture was sonicated at 25 kHz for 30 min to exfoliate rGO. The solution was filtered using 0.45 Polytetrafluoroethylene (PTFE) filters to remove un-exfoliated graphite and other debris [17].

Chitosan Extraction

Four stages were followed during chitosan extraction process. They are pre-treatment stage, demineralization, deprotonation and deacetylation stages. The squid gladii were collected along the Kilifi coastal beaches (Kenya) and washed to remove external matter. This was followed by sun drying for four days. 10 g of the

dry gladii were soaked in 50 ml of 0.01M NaOH solution at room temperatures for about 1 hour to remove non-chitin rich organic material. Here, also a small amount of proteins was removed. The pre-treated squid gladii were washed and sundried for two days, then grounded into fine powder (1.5 mm). 8 g of powder was soaked in 80 ml of 1M HCl solution at a temperature of about 60°C for 3 hours to dissolve minerals. Demineralized powder was filtered off the acidic solution and rinsed three times with distilled water. Deprotonation process was aided to remove the proteins from the demineralized gladii powder. This was done by soaking the washed powder in 0.125M NaOH at 70°C overnight. Once the deprotonation step was complete, the remaining component was the biopolymer chitin. The obtained chitin was washed till neutral PH using distilled water, then filtered to obtain chitin powder. Filtered chitin was dried in a hot air oven at 60°C for about 5 hours. The final step was deacetylation; conversion of chitin to chitosan. This was achieved by boiling the demineralized chitin powder in 1.25M NaOH solution at a 100°C for six hours. This was repeated thrice to obtain high deacetylated chitosan. The powder was then washed severally in distilled water until neutral pH. A white solid, chitosan, was obtained. The extracted chitosan was washed in alcohol to dissolve any non-chitosan compound. 0.01 g of the extracted chitosan was dissolved in 1% acetic acid and left to shake overnight in a warm water bath (about 50°C) to obtain chitosan solution.

rGO/Chitosan Blend and Film Preparation

1 ml of rGO solution each was measured into a clean glass vial. 1 ml of chitosan solution to vial was then added to the rGO solution to make 50% blend solution. The two vials were left shaking for 3 hours under a water bath at 50°C [18]. The films were prepared by spin coating method at 1500 rpm for 30 second on glass substrates.

Results and Discussion

Morphology of rGO Films

The bright field and birefringence micrographs of the blend films were obtained using the Zeiss Axio 100 microscope fitted with LCD camera (Germany). Figure (a), (b), and (c) shows the bright field images of the prepared film at different locations, while figures (d), (e) and (f) shows their respective birefringence images as observed under crossed polarisers. The films showed higher birefringence, with clear star-like crystallite structures.

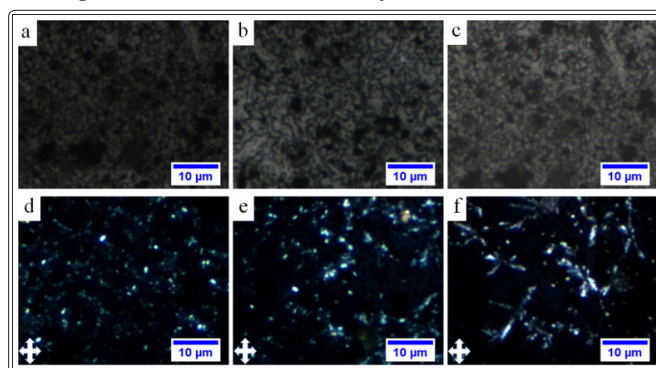


Figure 1: Micrographs of rGO films prepared by spin coating method at 1500 rpm for 30 seconds. Figures a, b, and c shows the bright field images of the film at different locations, while Figures d, e and f shows their respective birefringence images

Effect of Temperatures on Molecular Ordering of rGO Film Structures

The birefringence micrographs of the prepared rGO film were obtained using optical microscope under crossed polarizers. The films were subjected to heating up to about 120°C , followed by

subsequent cooling back to room temperature. The micrographs were taken at different temperatures during these processes. Figure 2 shows effect of temperature change on the crystal orientations of the rGO film.

As shown in the figure 2, the birefringence intensity decreased during the heating process, and completely disappeared at about 100°C. On cooling the film, birefringence re-emerged at about 90°C, and their intensities increased gradually as the temperatures were being cooled back to room temperature. Decrease in the birefringence intensity with increasing temperature was due to reduction in the degree of crystal order. This can simply be explained in the basis of disorientation of dipole moments. Temperature can alter the anisotropy.

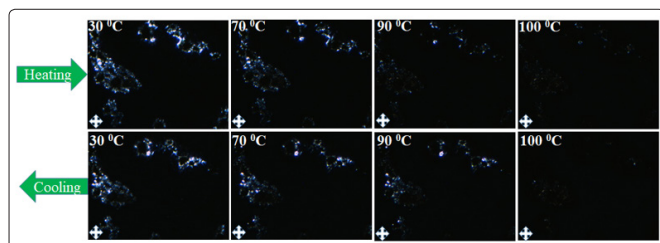


Figure 2: Micrographs showing effect of temperatures on molecular ordering of rGO crystallites. (Image size 68x52 μm)

Heating the film resulted in vibration of the rGO molecules due to increased molecular kinetic energy, which resulted in dis-orientation of the dipole moments. The disappearance of birefringence at 100 °C implied that the rGO molecular order was completely destroyed. Here, the dipole moments were oriented in different directions, with no particular defined order. On cooling, the birefringence reappears at about 90 °C, and their intensity increased with further cooling. Cooling reduced the molecular kinetic energy, thus the dipoles moments regained their initial stability.

Morphologies of rGO/Chitosan Blend Films

Figure 3 (a), (b) and (c) shows the bright field images of the blend film at different locations, while (d), (e) and (f) are their respective birefringent images

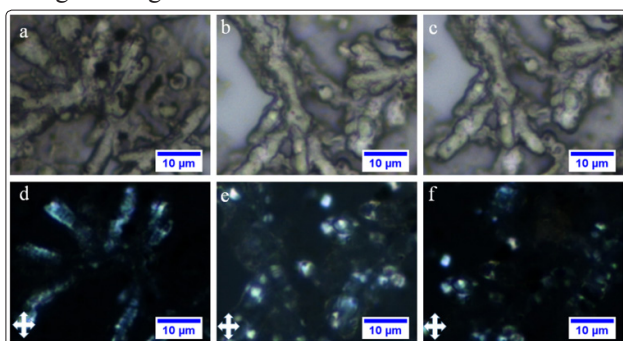


Figure 3: Micrographs showing dendritic structures of rGO/Chitosan blend (50%) spin coated film at different locations on the same film. Figure (a), (b) and (c) shows the bright field images while (d), (e) and (f) are their respective birefringent images

As shown in Figure 3, clear dendritic structures were obtained. The formation of dendritic structures was due to spontaneous nucleation that was induced by rGO, resulting in uneven growth of the blend crystals. On viewing the film under crossed polarized light, the birefringence was observed along the tendrils. rGO induced chitosan polymer nucleation, and after a stable growth front was formed, structural growth began. Chitosan molecules

approached and attached themselves to a stable seed, resulting in structural growth. The structured grew along the dendrites, which are the nucleation sites.

Conclusion

From this study, it was observed that rGO induced chitosan crystallization, which led to formation of dendritic structures. rGO films showed relatively higher birefringence, which decreased in intensity during temperature increase, but regained its initial formations on cooling. Structural growth was observed along the dendrites, which were believed to be the nucleation sites.

Acknowledgements

We would like to extend our sincere gratitude to Pwani University and Jaramogi Oginga Odinga University of Science and Technology (JOUST) fraternities for availing basic equipment for this research.

References

1. Y Fu, Z Kang, J Yin, W Cao, Y Tu, et al. (2019) The Duet of Acetate and Water at the Defects of Metal-Organic Frameworks. *Nano Lett* 19: 1618-1624.
2. C Kastl, RJ Koch, CT Chen, J Eichhorn, S Ulstrup, et al. (2019) Effects of Defects on Band Structure and Excitons in WS₂ Revealed by Nanoscale Photoemission Spectroscopy. *ASC nano* 13: 1284-1291.
3. H Li, L Han, J Hou, J Liu, Y Zhang (2018) Oriented Zeolitic Imidazolate Framework Membranes within Polymeric Matrices for Effective N₂/CO₂ Separation. *J Memb Sci* 572: 82-91.
4. S Daniel, K Hartmut, M Fanuel, K Susanna, H Ralf, et al. (2016) Poly(3-(2,5 ioctylphenyl)Thiophene) Synthesized by Direct Arylation Polycondensation. End Groups, Defects, and Crystallinity *Macromolecules* 49: 7230-7237
5. GC Efe, I Altinsoy, S Türk, C Bindal, AH Ucisik (2019) Effect of Particle Size on Microstructural and Mechanical Properties of UHMWPE -TiO₂ Composites Produced by Gelation and Crystallization Method. *J Appl Polym Sci* 136: 15-18.
6. RH Doremus, BW Roberts, DTurnbu (2007) Book Review. *J Polym Sci* 133: 2053-2054.
7. PH Till (1957) The Growth of Single Crystals of Linear Polyethylene. *J Polym Sci* 106: 301-306.
8. P Welch, M Muthukumar (2001) Molecular Mechanisms of Polymer Crystallization from Solution. *Physical Review Letters*. 87: 19-22.
9. G Strobl (2007) The Physics of Polymers-Concepts for Understanding Their Structures and Behaviors. *Lect Notes Phys* 714: 87-96.
10. I Tsigos, A Martinou, D Kafetzopoulos, V Bouriotis (2000) Chitin Deacetylases :New , Versatile Tools In. *TIB Technol* 18: 305-312.
11. M Maria S, Gadelha, TCM Stamford, E Pereira, P Tenório, et al. (2011) Chitosan as an Oral Antimicrobial Agent. *Sci against Microb Pathog Commun Curr Res Technol Adv* 542-550.
12. RCF Cheung, TB Ng, JH. Wong, WY.Chan (2015) Chitosan: An Update on Potential Biomedical and Pharmaceutical Applications. *Mar. Drugs* 13: 5156-5186.
13. D Sugiyanti, P Darmadji, S Anggrahini, C Anwar, U Santoso (2018) Preparation and Characterization of Chitosan from Indonesian Tambak Lorok Shrimp Shell Waste and Crab Shell Waste Pakistan. *J Nutr* 17: 446-453.
14. X Duan, B Yu, T Yang, Y Wu, H Yu, T Huang (2018) In Situ Polymerization of Nylon 66 / Reduced Graphene Oxide Nanocomposites. *J Nanomater.* 6: 1-9.

15. J Wang, MW Ellsworth (2014) Graphene and Graphene Oxide Aerogels. Google Patents 3: 1-6.
16. K Wardhani, IMA Nugraha, S Abidin, M Ali, A Fahmi (2017) Solution of Reduced Graphene Oxide Synthesized from Coconut Shells and Its Optical Properties. 3rd Int Conf Adv Mater.Sci Technol 020045: 1-8.
17. E Sulistyani, D Boi, F Wulandari, E Budi (2015) Coconut Shell Activated Carbon as an Alternative Renewable Energy. Renew. energy Energy Conserv. Exhibition 2:76-81.
18. S Xu, Y Zhang, K Dong, J Wen, C Zheng, S Zhao (2017) Electrochemical DNA Biosensor Based on Graphene Oxide-Chitosan Hybrid Nanocomposites for Detection of Escherichia Coli O157 : H7. Int. J Electrochem Sci 12: 3443-3458.

Copyright: ©2021 Agumba O John, et al. This is an open-access article distributed under the terms of the Creative Commons Attribution License, which permits unrestricted use, distribution, and reproduction in any medium, provided the original author and source are credited.